Design of Structure for a Heavy Duty Mineral Tow Machine by Evaluating the Dynamic and Static Loads

Mehdi Akhondizadeh[1], Meysam Atashafrooz[2], *

Department of Mechanical Engineering
Sirjan University of Technology, Sirjan, Iran
E-mail: m.akhondizadeh@sirjantech.ac.ir, m.atashafrooz@sirjantech.ac.ir,
Meysam.atashafrooz@yahoo.com
*Corresponding author

Abstract: The present manuscript gives the description of findings which took importance during the design and analysis of the structure of heavy duty hauler machine ordered by Gol-e-Gohar iron ore complex in Iran. Stress and deformation analysis was indeed the heart of the project and the key of its success. The challenging problem of evaluation of value and behaviour of active loads was taken under consideration precisely and all participated external forces were included in analysis. Since the present case is a moving structure, the loading evaluation should be included in all critical experienced conditions through the operation. The inertial forces due to acceleration and road bump have the governing role and have been evaluated and considered in analysis. After precise and complete evaluation of external loads and applying the correct boundary conditions, the simulations for stress analysis have been performed in ANSYS. The main findings of the present study were the optimized decision for the geometry of several important load carrying elements and appropriate reinforcement of the risky positions which was the result of the correct knowledge of the mechanics of problem. Finally, the structure was manufactured with the total weight of about 38 ton and load carrying capacity of 120 ton including the dynamic effects. After succeeding in the initial loading, the operational loading in real conditions in mine ramp has been carried out gradually and the machine is currently working in desired predicted form.

Keywords: Dynamic Load, Mechanical Design, Static Load, Stress Analysis, Tow Structure

Biographical notes: Mehdi Akhondizadeh is an assistant professor of Mechanical Engineering in Sirjan University of Technology, Sirjan, Iran. He received his MSc and PhD degrees from Shahid Bahonar University of Kerman in 2009 and 2015, respectively. He has several published papers and researches about the computational and experimental mechanics. **Meysam Atashafrooz** is an associate professor of Mechanical Engineering in Sirjan University of Technology, Sirjan, Iran. He received his MSc and PhD degrees from Shahid Bahonar University of Kerman in 2011 and 2015, respectively. He has several published papers about the computational mechanics and CFD research area.

Research paper

1 INTRODUCTION

Design of the machines requires a range of the engineering knowledge including the load analysis, material knowledge, drawing, stress analysis, cost evaluation and etc. The mechanical engineering knowledge has the higher degree of importance in the design of the heavy duty machines. The factors of style and cost of machines is not as important as the strength of the machine for working in the rough conditions in mine. The experiment-based findings will be very helpful in mechanical engineering design.

Shigley's mechanical engineering design [1] is full of such relations which simplifies the decisions for the engineers. The research results to be usable for all should be described in same language [2]. The computer aid design gradually finds its way into the engineering design by the modelling and analysing programs and software [3]. Computers also simplified the material selection [4]. Mineral machinery has the heaviest duty and so require the thorough load and stress analysis to select the optimized dimensions to have the minimum weight for the required application. Si et al. [5] analysed the force of frame in the dump truck unloading. ANSYS analyses indicated the stress concentration region to enhance it. Yi Dengli [6] analysed the models of tank car in ANSYS to determine the effect of thickness and height of the wave preventer on the deformation, strain and stress under different working conditions to optimize the dimension of elements. Cao et al. [7] performed FEM analysis for the frame of the truck crane. Results showed that the maximum stress is beyond the yield strength which requires the improvement of the frame structure. Through the load analysis of heavy vehicles, the dynamic force due to cross over road bump should be evaluated to determine its importance [8-9]. There are approaches for evaluating this form of loading on vehicle structure and human [10-12]. From the other point of view, choice of the enhanced materials will reduce the total weight and failure risks [13]. However, the cost considerations should be evaluated.

In the present work, it is tried to design a structure for climbing the mineral machinery to transport them in a faster and lower cost way in mine. The effort was paid to precisely determine the static and dynamic loads to have more reliable design. The novelty of work is application of the dynamic relations to evaluate the additional load due to the crossing the machine over the road bump which is one of the main parts of the loading which is precisely took in account here.

2 DESCRIPTION OF NEED

The availability of heavy mineral machines is one of the most important factors in improving the productivity of mineral processing. The term "walking of the machinery" is used when a mineral machine has to travel a relatively long distance through the mine environment. It is not welcomed by industries due to the time wasting and inherent costs and the effort is to avoid of it. The alternative of the walking will be conveying the slow and heavy machines by a faster and lower cost way. The design of a vehicle having such ability was on the agenda.

3 GEOMETRY LAYOUT

The final geometry of any design is the outcome of the designer viewpoint, manufacturing abilities, cost, functionality, experience, inspiring from similar designs and etc. According to these aspects, the present geometry was finalized which requires to be manufactured at another shop and conveyed to the owner company. Planned layout was decided to have the configuration to be built in separate conveyable structures. After assessment, evaluation and discussion, the general schematic of structure was gradually specified. The final decision was that it would compose of five main structures including two side-structures, central structure, axle structure and Jumbo structure.

4 LOADING SUMMARY AND ITS PATH

The loading of the present structure comes of the carrying of a mineral machine, for example an excavator, which its chain wheels insert the excavator weight on the side-structure of the tow machine. The side structures transfer the load to the central structure by the connecting pins. The load then is divided in two parts by transferring from the central structure to the axle from the rear and to the Jumbo from the front. The graphic summary of the approximate path of transferring the excavator weight to the ground, through the tow structure, has been illustrated in "Fig. 1".

The loading initiates from the weight of the excavator (w) which produces F_1 and M_1 at the support of the first load carrying elements of side structure. Intermediate supports were designed in the central structure to take the major component of M_1 on their both sides. They prevent these couples to be applied on the base plate of the central structure. F_1 transfers and distributes on the base plate of the central structure through F_3 and F_4. F_3 and F_4 then transfer to the Jumbo and axle by F_5 and F_6, respectively.
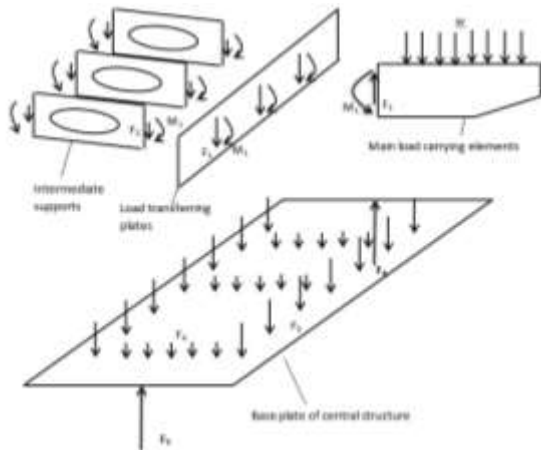
Fig. 1   Load trend from source to the axle.

More evaluations indicated that the structure weight has the noticeable value compared to the design external load. So, the effort was paid on optimizing the structure from the weight point of view to have the maximum strength by the minimum weight. The main load carrying parts were the elements in side-structure which must get the load from the wheels of target machine and transfer it to the central structure. Several choices for these parts, as illustrated in "Fig. 2", have been analysed by ANSYS software to obtain the best choice.
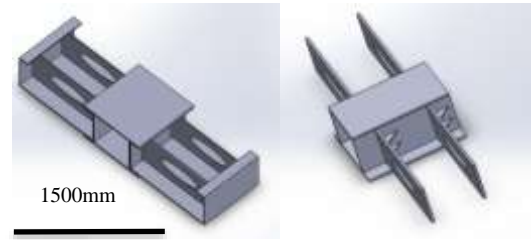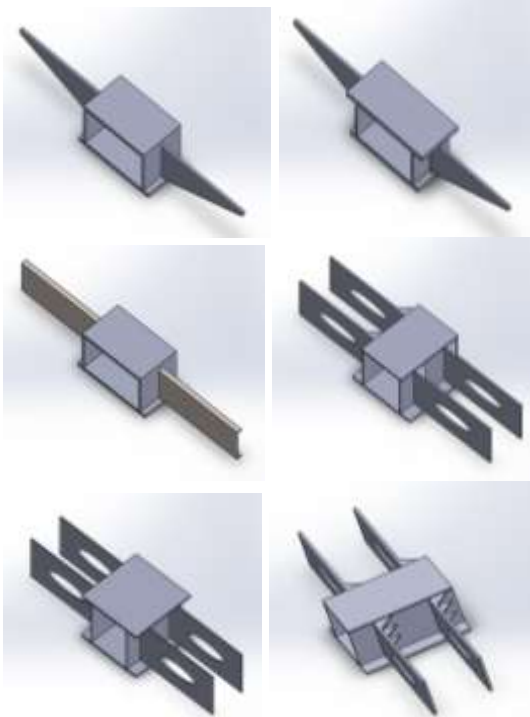
Fig. 2   Elementary options for the main load carrying elements.

The final choice for the main load carrying elements after analyses was as illustrated in "Fig. 3". Since it must have the maximum bending strength, its top and bottom faces were reinforced by small plates. They were also strengthened by additional elements at the support end which must be welded to the central structure.
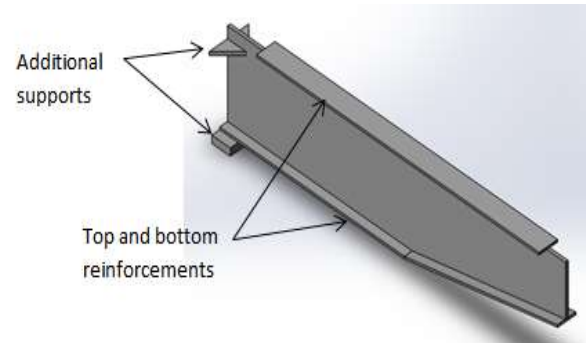

Fig. 3   The final choice for the main load carrying part.

From one end, the main load carrying elements of the side structure are welded on a plate which is considered to be pinned to another plate on the central structure. They are welded to a C-type beam from the other end to compose the rigid side structure. The central structure was reinforced by the intermediate elements which increase its stability. The final design of the combination of the side and central structure has been illustrated in "Fig. 4".

Fig. 4   The final design of the main structure.

5   DESIGN LOAD

The design load is evaluated based on the specifications of CAT390DL hydraulic excavator which its dimension and center of mass of parts are illustrated in "Fig. 5" and their values are given in "Table 1". The total mass of excavator is about 80ton which is applied on the different parts of the main structure through the climbing, positioning in place on side structures, accelerating and decelerating in the mine ramp and crossing over road bump.
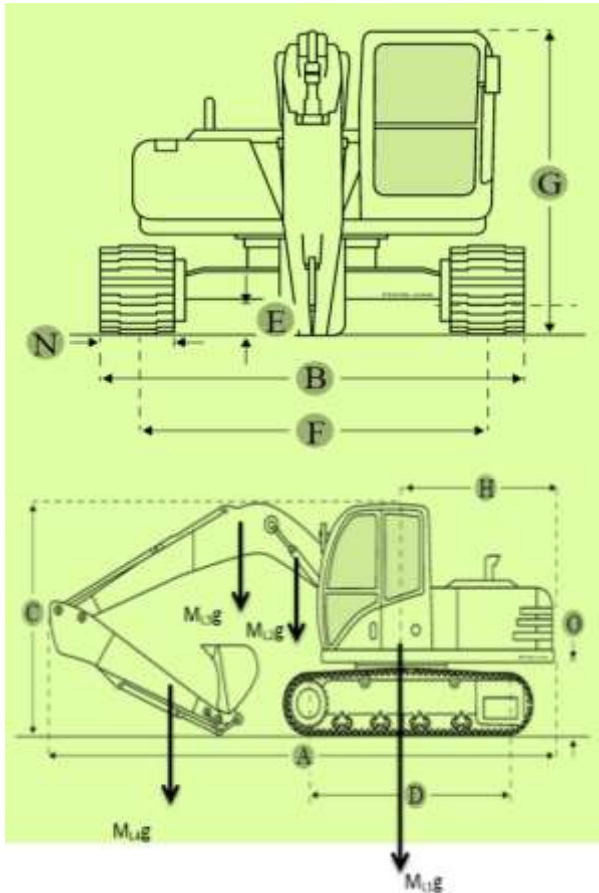

Fig. 5   Specific dimensions and center of mass of parts of CAT390DL hydraulic excavator.

Table 1 Values of specific dimensions and mass of parts of CAT390DL hydraulic excavator

Parameter Name	Value
A	12 m
B	4.6 m
C	3.76 m
D	5.12 m
N	0.9 m
M_{L1}	68 ton
M_{L2}	1.7 ton
M_{L3}	9.7 ton
M_{L4}	5.43 ton

The inertial forces must be included in the applied loads which can be described in two forms: accelerating through the mine ramp and crossing over the road bumps. The schematic of the form of applying these inertial forces is illustrated in "Figs. 6 and 7".
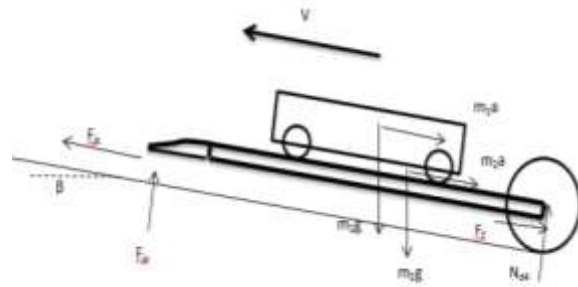

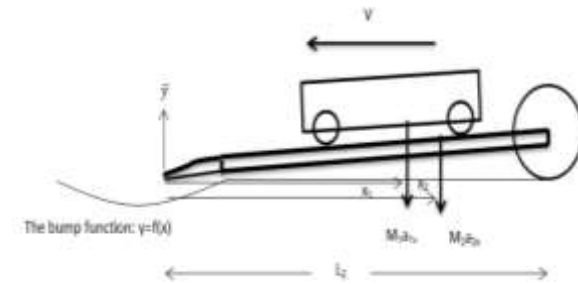**Fig. 6**   Force diagram through accelerating of tow at the mine slope.

Fig. 7   Inertial forces due to the cross over road bumps.

Obviously, the linear acceleration due to the velocity increment during the motion of the tow does not have a constant value. However, an estimation of inertial force for stress analysis purpose will be obtained by assuming the constant acceleration. The velocity increment Δv over the time Δt gives a constant acceleration as follow:

$$a = \frac{\Delta v}{\Delta t} \tag{1}$$

The other noticeable inertial force will be due to the cross over the road bump. The form of this inertial force, as illustrated in "Fig. 7", is such that the front head of structure experiences a sudden downward-upward motion at the small period of time. It induces a semi-shock force on the target machine and the structure of the conveying machine. The influence of the road bump on the inertial force can be described by the following relations with the help of schematic illustrated in "Fig. 7".

$$Y = f(x) \tag{2}$$
$$\dot{y} = \dot{x}\frac{\partial f}{\partial x} \tag{3}$$

$$\ddot{y} = \ddot{x}\frac{\partial f}{\partial x} + \dot{x}^2 \frac{\partial^2 f}{\partial x^2} \qquad (4)$$

Assumption:

$$\ddot{x} = 0 \qquad (5)$$

Assumption: small structure incline, angular acceleration is:

$$\alpha = \frac{\ddot{y}}{L_2} \qquad (6)$$

$$a_{1y} = (L_2 - x_1)\alpha \qquad (7)$$

$$a_{2y} = (L_2 - x_2)\alpha \qquad (8)$$

Numerical calculation of the acceleration and inertial force due to the road bump requires an assumed function $f(x)$. The common shape of most road bumps can be estimated by a sector of circle as illustrated in "Fig. 8".
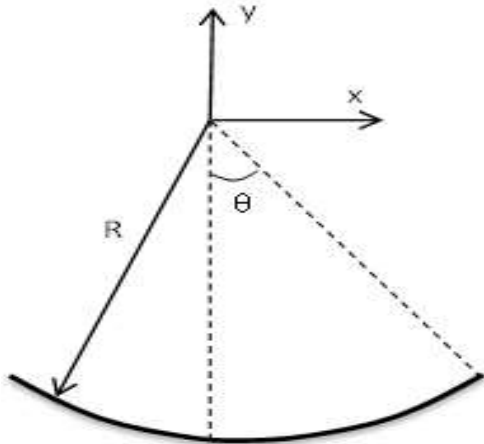
Fig. 8 The sector of circle as the road bump.

$$y = -\sqrt{R^2 - x^2} \qquad (9)$$

$$\dot{y} = -\frac{1}{2}(-2x\dot{x})(R^2 - x^2)^{-\frac{1}{2}} \qquad (10)$$

$$\ddot{y} = (\dot{x}^2 + x\ddot{x})(R^2 - x^2)^{-\frac{1}{2}} + x\dot{x}\left(-\frac{1}{2}\right)(-2x\dot{x})(R^2 - x^2)^{-\frac{3}{2}} \qquad (11)$$

$$\dot{x} = -v, \quad \ddot{x} = 0 \qquad (12)$$

$$\ddot{y} = \dot{x}^2(R^2 - x^2)^{-\frac{1}{2}} + x^2\dot{x}^2(R^2 - x^2)^{-\frac{3}{2}} \qquad (13)$$

The required parameters and numerical results of the acceleration evaluation are given in "Table 2".

Table 2 Design parameters

Parameter	Value	Parameter	Value
M1(External Load)	80 ton	R	6
M2 (Structure)	30ton	θ	60º
L1 (m)	5.12	v	22km/h
L2 (m)	12.5	a_{1y}	0.56g
X_1(m)	4.5	m/s²	
X_2	7	a_{2y}	0.58g
X_3	6.25	m/s²	
β	10º	Δv	30km/h
		Δt	30s
		a	0.1m/s²

6 FINAL LOADING

Not all features of the static and dynamic loads have been cleared. The complete form of the machine was also specified by the partly analyses and decisions. The applied loads and reactions of the axle and Jumbo have been illustrated on the final shape of machine in "Fig. 9". In this figure, F_1 represents the weight of the conveyed machine (excavator) and the dynamic force $M_1 a_{1y}$ and F_2 represents the inertial force $M_1 a$. Moreover, the weight of the structure and its inertial force are distributed over the whole structure as the body force.
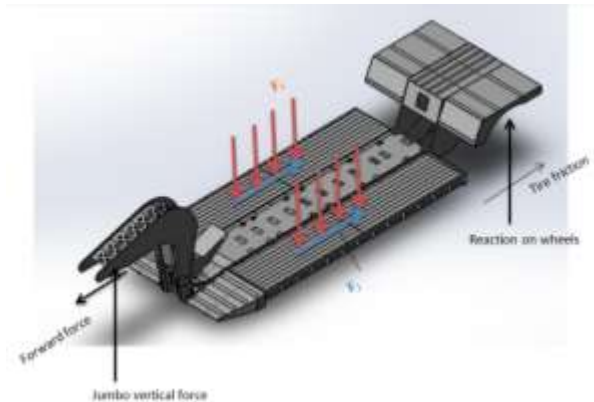

Fig. 9 Force free diagram of external loads on tow structure.

7 LOAD TRANSFERRING ELEMENTS

The form of action of the mechanical elements is described here. The dimension and position of all of elements have been selected such that their maximum load carrying capacity is employed during the different stages of loading. The side structure which is the first component that receives the load has three main parts

including load carrying elements, reinforcing C-type beam and support plate. This beam has the role of load distributing between the main load carrying elements. Without this beam, while the external load receives the first main carrying elements due to the movement of carried machine on the hauler structure, the non-loaded carrying elements do not participate in load carrying and this has the risk of failure of the first carrying elements. At the first stage, the load is applied on the load carrying elements and transfers through it to the support plate to be delivered to the central structure. The elements 1, 2, 3, …, q ("Fig. 10") directly receive the load during the climbing and sitting the excavator on the structure whereas, elements q to N may never directly experience the load but they have the significant effect in increasing the overall strength and stiffness of whole of the side structure by supporting the reinforcing beam.
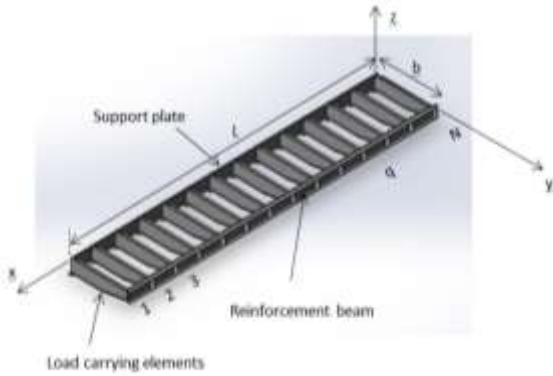

Fig. 10 The main components of the Side structure.

Due to the importance of the main load carrying elements their reaction under loading is discussed in more detail to clear how it transfers the load to the other elements. The deformed shape of these elements after loading is exaggeratedly illustrated in "Fig. 11" and can be given as follow:

$$\vec{U} = u(x,y,z)\vec{i} + v(x,y,z)\vec{j} + w(x,y,z)\vec{k} \qquad (14)$$
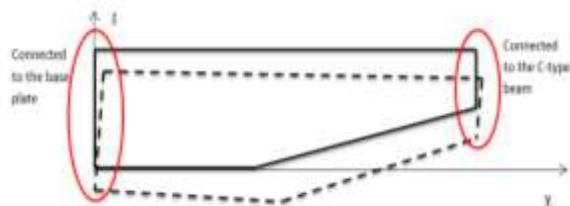

Fig. 11 Exaggerated deformation of the main load carrying element of the side structure.

The base plate and reinforcing beam must show resistant to the displacement at the left and right edges

of the main load carrying elements. Such view of the action of the elements will help to appropriate and optimized selection of their type and dimension. The base plate must have the maximum stability under the rotation about the *x*-axis whereas, the reinforcing beam is required to withstand the displacement at the *x* and *z* directions. The base plate is pinned to the central structure at the appropriate regions to have this ability at its best form and the reinforcing beam gets the load from the active load carrying elements (1…q) and transfers it to the inactive ones (q…N) to engage them in the load carrying. This explanation is completed by the force diagram which is illustrated in "Fig. 12".
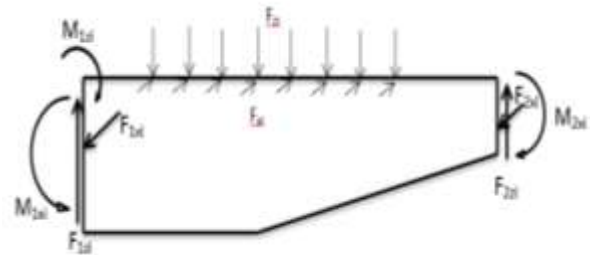

Fig. 12 The force diagram of the main load carrying element of the side structure.

The following relations can be explained by the reactions mathematically:

$$M_{2xi} \propto \frac{\partial v(x,b,z)}{\partial z} \qquad (15)$$

$$F_{2zi} \propto \frac{\partial w(x,b,z)}{\partial x} \qquad (16)$$

$$F_{2xi} \propto \frac{\partial u(x,b,z)}{\partial x} \qquad (17)$$

Based to the described requirements, a C-type beam reinforced against torsion by the small elements as illustrated in "Fig. 13" will give the desired performance in increasing the rigidity of side structure under the heavy weight of external load.
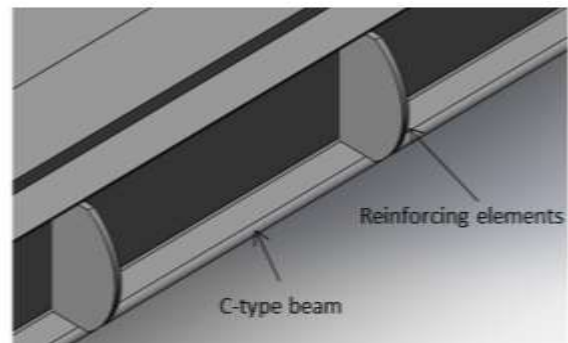

Fig. 13 Reinforcing elements of the c-type beam.

8   CONNECTION OF SIDE STRUCTURE TO THE CENTRAL STRUCTURE

As discussed previously, the required reactions on the connection of side and central structures are M_{1zi}, M_{1xi}, F_{1xi}, F_{1zi} which distribute discretely over the x-axis where there exist a load carrying element. These loads transfer between two steel plates of side and central structures, connected by 6 metric bolts $M_{64 \times 6}$ grade10.9 spaced *2m* over the length of the structure. Configuration of the elements and connections is such that the minor part of these loads is received by the base plate of the central structure.

The nature of loads directs the designers to consider the intermediate elements in the central structure which are welded from both sides to the connecting plates to provide their stability and increase the rigidity of the central structure. The configuration is such that the main loads applied on these elements are bending moments from the both sides. (See "Fig. 14").
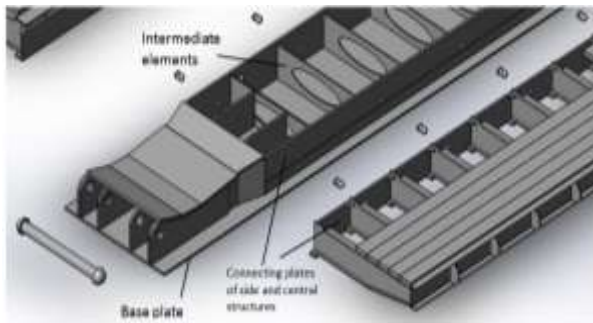

Fig. 14   Active load transferring elements.

9   STRESS ANALYSIS

After the selection of the load carrying elements and indication of the load values, the stress analysis has been performed in ANSYS software. The schematic of loading corresponding to the case in which the machine moves upward on the mine ramp of 10º and also crosses over an assumed road bump has been illustrated in "Fig. 15".

Fig. 15   The schematic of loading for analysis in ANSYS.

In "Fig. 15", *A* represents the side where the central structure is lifted by Jumbo and *B* represents the axle side. The boundary conditions are as follow:

At A: $U_x = U_y = U_z = 0$ (18)

At B: $U_y = U_z = 0$ (19)

The 8 mm mesh is illustrated in "Fig. 16". The contour of stress and deflection of the whole structure is illustrated in "Figs. 17 and 18", respectively.
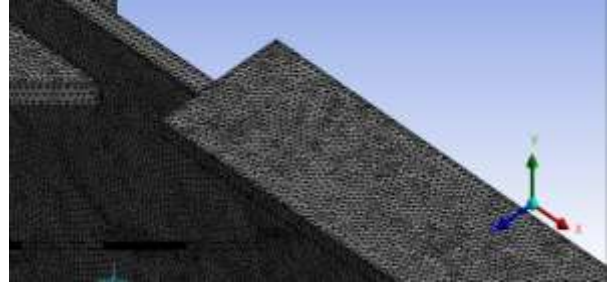

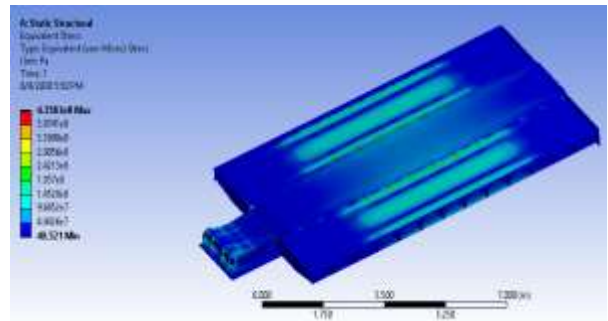**Fig. 16**   Mesh of the structure.
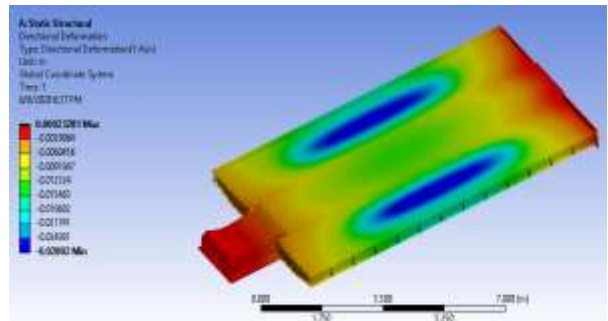

Fig. 17   Stress contour of the structure.

Fig. 18   Deflection of the structure at direction of y.

The results of the finite element analysis indicated that the maximum stress in structure is about 435MPa which is beyond the minimum yield strength of 335MPa of the structure material St52. Extracting the maximum stress of the individual elements which are given in Table 3 revealed that this is not a problem. The maximum stress is lower than the yield strength for all parts except for the connecting elements of the central structure to the jumbo. At this region, the stress concentration at pin holes occurs. Practically, these stresses will be relieved after local plastic deformations.
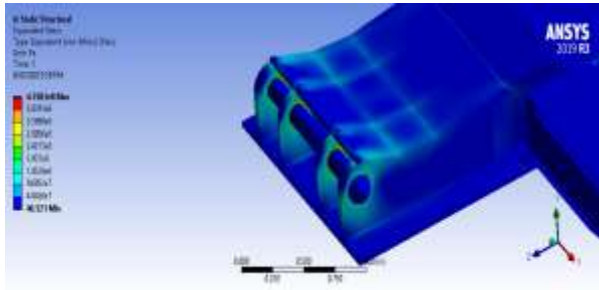
Fig. 19   Stress concentration regions.

Table 3 Values of the maximum stress at individual parts

Part	Max. Stress (MPa)
Main load carrying	174
Connection Side plate	188
Connection pins	89
Central base plate	182
Connection central plate	284
Intermediate supports	119
Pin Jumbo	240
C-type beam	100

Table 4 Load values (kN) of Figure 20

W	F$_1$	F$_2$	F$_3$	F$_4$	F$_5$	F$_6$	F$_7$
1224	563	614	319	1010	351	268	108

The stress analysis has been done and stress contour has been illustrated in "Fig. 21".
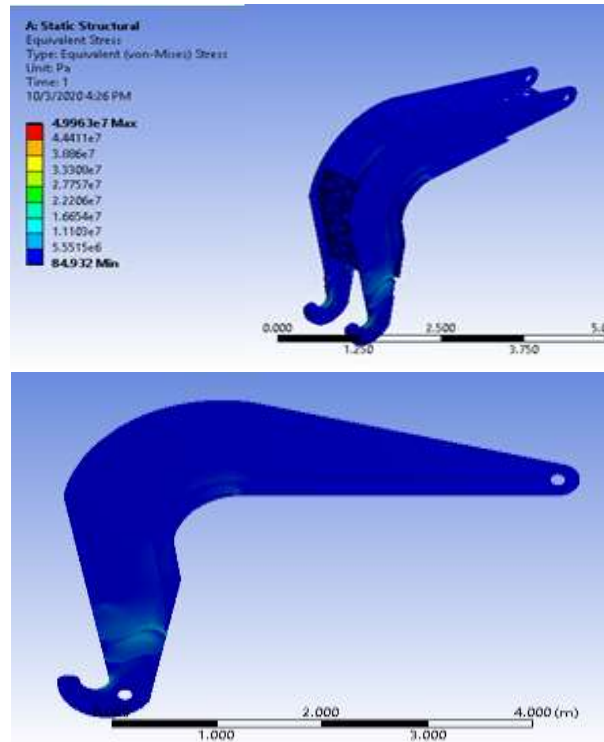
Fig. 21   The stress contour of the Jumbo structure.

The simulations showed that the stress values in jumbo are acceptable. The maximum stress at the stress concentration regions is 49MPa. So, it says that there is no problem for jumbo.

Jumbo is another component of the present structure which is composed of the several individual parts and requires load and stress analysis. Jumbo has the role of lifting the head of the main structure by hydraulic pressure after loading. It also transfers the driving force from the haul truck to the main structure during the accelerating. The force diagram of the combination of the main structure and Jumbo has been illustrated in "Fig. 20" which shows how loads apply on Jumbo.
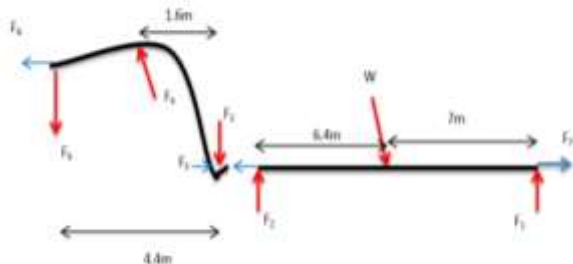

Fig. 20   Force diagram of whole structure with Jumbo.

The jumbo sits on a flat base on haul truck where F_4 is applied. Elsewhere the revolute joint between the haul truck and jumbo produces F_5 and F_6. In fact, F$_6$ is the driving force which provides the requirements for accelerating the main structure and tire friction. For analysis, the region on which F_4 has been distributed is constrained as $U_y=U_z=0$ and the revolute joint is constrained as $U_x=U_y=U_z=0$. The values of loads are given in "Table 4".

10   CONCLUSION

After the appropriate definition of need for the faster transportation of the mineral machinery, the load analysis and load carrying element selection were performed based on a specified external load. A variety of conditions were taken into account to determine the critical loading condition. Individual stress analysis leads the designer to the appropriate dimension of elements. After that, the 3D model of whole structure was made in Solid works software and was analyzed in ANSYS. The result was the structure which currently passes the initial field tests as illustrated in "Fig. 22" in which the structure conveys a mineral truck of about 70% of the design load.

Fig. 22   Field test of the structure by 70% of design load.

ACKNOWLEDGMENT

REFERENCES

[1] Budynas, R. G., Nisbett, J. K., Shigley's Mechanical Engineering Design, New York: McGraw-Hill, Vol. 9, 2011.

[2] Finger, S., Dixon, J. R., A Review of Research in Mechanical Engineering Design. Part I: Descriptive, Prescriptive, and Computer-Based Models of Design Processes, Research in Engineering Design, Vol. 1, No. 1, 1989, pp. 51-67.

[3] Ullman, D. G., Toward the Ideal Mechanical Engineering Design Support System, Research in Engineering Design, Vol. 13, No. 2, 2002, pp. 55-64.

[4] Sapuan, S. M., A Knowledge-Based System for Materials Selection in Mechanical Engineering Design, Materials & Design, Vol. 22, No. 8, 2001, pp. 687-695.

[5] Si, J. P., Wang, G. S., and Ding, X. L., Analysis of Dump Truck Unloading Condition Based on ANSYS, In Advanced Materials Research, Vol. 548, 2012, pp. 724-729.

[6] Yi, D., Strength Analysis and Optimization of Tank Truck Based on ANSYS, In Journal of Physics: Conference Series, Vol. 2026, No. 1, 2021, pp. 012058.

[7] Cao, F., Li, J., and Cui, M., Analysis of Frame Structure of Medium and Small Truck Crane, In AIP Conference Proceedings, Vol. 1944, No. 1, 2018, pp. 020065.

[8] Startcev, A., Romanov, S., and Vagina, O., Interaction of Elastic Wheel with Bumps of Rectangular Shape. In International Conference on Industrial Engineering, Springer, Cham, 2019, pp. 621-629.

[9] Desai, R., Guha, A., and Seshu, P., Investigation of Internal Human Body Dynamic Forces Developed During a Vehicle Ride, In the International Conference of IFToMM ITALY, Springer, Cham, 2020, pp. 85-93.

[10] Goenaga, B., Underwood, S., and Fuentes, L., Effect of Speed Bumps on Pavement Condition, Transportation Research Record, Vol. 2674, No. 9, 2020, pp. 66-82.

[11] Tengler, S., Warwas, K., An Effective Algorithm of Uneven Road Surface Modeling and Calculating Reaction Forces for a Vehicle Dynamics Simulation, Coatings, Vol. 11, No. 5, 2021, pp. 535.

[12] Guo, Z., Wu, W., and Yuan, S., Longitudinal-Vertical Dynamics of Wheeled Vehicle under Off-Road Conditions, Vehicle System Dynamics, Vol. 60, No. 2, 2022, pp. 470-490.

[13] Vini, M. H., Daneshmand, S., Effect of Electrically Assisted Accumulative Roll Bonding (EARB) Process on the Mechanical Properties and Microstructure Evolution of AA5083/Al2O3 Composites, Materials Performance and Characterization, Vol. 8, No. 1, 2019, pp. 594-603.